Pr doped bismuth ferrite ceramics with enhanced multiferroic properties

P Uniyal and K L Yadav

Department of Physics, Indian Institute of Technology Roorkee, Roorkee 247667, India

E-mail: klyadav35@yahoo.com

Abstract
Pr modified $Bi_{0.9-x}La_{0.1}Pr_xFeO_3$ (BLPFO-x, $x = 0$, 0.1 and 0.2) ceramics were prepared by the conventional method based on the solid state reaction of mixed oxides and a detailed study of electrical and magnetic properties of Pr modified bismuth ferrite (BLPFO) is reported. X-ray analysis shows the formation of a bismuth ferrite rhombohedral phase. Pr doping significantly increases the resistivity and leads to a successful observation of electrical polarization hysteresis loops. All the samples have been found to possess a spontaneous magnetic moment at room temperature which increases further at low temperatures. The strong dependence of remnant polarization and dielectric constant on the strength of magnetic field is a direct evidence of magnetoelectric coupling in BLPFO-2 ceramics.

(Some figures in this article are in colour only in the electronic version)

1. Introduction

In recent years, great attention has been paid to multiferroics due to the potential applications for new electronic devices as well as the fascinating fundamental physics. These materials simultaneously show spontaneous electric and magnetic ordering in the same phase [1]. These materials may also exhibit attractive functionalities caused by the interaction between electric polarization and magnetization (magnetoelectric effect) [2]. Bismuth ferrite posses a polarization (ferroelectric) ordering with a high Curie temperature T_C of 1103 K and a spin (antiferromagnetic) ordering of the G type with a magnetic transition temperature T_N of 643 K. Superimposed on this antiferromagnetic ordering there is a cycloidal modulation with a wavelength of ∼62 nm [3]. Consequently, its remnant magnetization and potential magnetoelectric effect both vanish macroscopically, leading to a weak quadratic magnetoelectric behavior rather than a strong linear magnetoelectric behavior [4–6].

A spontaneous magnetization in $BiFeO_3$ has been observed due to partial ionic substitution to $BiFe_{1-x}M_xO_3$ (M is, typically, another 3d transition metal) and $Bi_{1-x}A_xFeO_3$ (A is a lanthanide ion, alkali earth metal or lead) and has been attributed to valence fluctuations between Fe^{2+} and Fe^{3+} ions or to spin canting [7–13]. But spontaneous polarization has always been difficult to obtain in bulk $BiFeO_3$-based multiferroics due to the large leakage conductivity which can significantly interfere with the measurement of ferroelectric hysteresis loops giving rise to artificially large polarization and hampering intrinsic polarization switching. A high P_s of 0.6 C m^{-2} has been obtained for single crystalline thin layers fabricated by pulsed laser deposition along the [001] and [111] directions at room temperature [14].

Benfang *et al* have reported the effect of Pr doping on the room temperature electrical and magnetic properties of $BiFeO_3$ thin films [15]. The dielectric and low temperature magnetic properties were not addressed at all. In the present paper we have synthesized Pr doped $BiFeO_3$, $Bi_{0.9-x}La_{0.1}Pr_xFeO_3$ (BLPFO-x) ceramics with $x = 0$, 0.1 and 0.2 by a standard solid state reaction method [13]. A small amount of lanthanum is added to stabilize the perovskite $BiFeO_3$ phase as reported by Palkar *et al* for Tb doped $BiFeO_3$ [16]. Pr has been used as a dopant with the idea that Pr_6O_{11} will reduce the conductivity of $BiFeO_3$ since it is a mixture of Pr^{3+} and Pr^{4+} ions. A systematic study of the effect of Pr doping on the structural, ferroelectric, dielectric and magnetic properties of $BiFeO_3$ has been reported. Also the magnetic field dependence of electric polarization has been studied in order to see the extent of magnetoelectric coupling in the system.

2. Experimental details

Polycrystalline BLPFO samples were prepared using reagents Bi_2O_3, La_2O_3, Fe_2O_3 and Pr_6O_{11} by a standard solid state
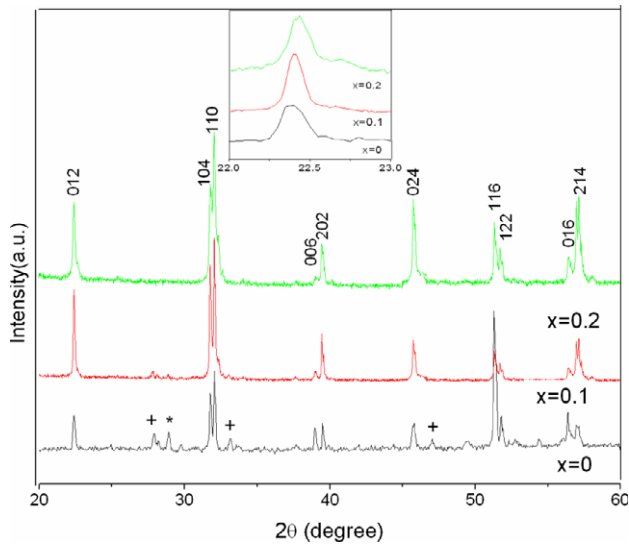
Figure 1. X-ray diffraction pattern for the $Bi_{0.9-x}La_{0.1}Pr_xFeO_3$, system ($x = 0, 0.1$ and 0.2), (+) and (*) represents the $Bi_2Fe_4O_7$ and $Bi_{46}Fe_2O_{72}$ impurity phases respectively. The inset shows the enlarged view of the [012] peak.

reaction method. The calcination was done at $820\,^\circ$C for 2 h. The x-ray diffraction pattern of the compounds was recorded at room temperature using an x-ray powder diffractometer (Brueker D8 Advance) with Cu Kα radiation (1.5418 Å) in a wide range of Bragg angles 2θ (20°–60°) at a scanning rate of 1° min^{-1}. The dielectric measurements were done using an automated HIOKI 3532-50 Hi Tester, LCR Meter. Magnetization data were collected using a superconducting quantum interference device (SQUID). The polarization–electric field (P–E) hysteresis loops were measured at room temperature by the modified Sawyer–Tower circuit (Automatic P–E loop tracer system, Marine India Electr. Pvt. Ltd). To study the magnetocapacitance measurement, a Wayne Kerr 6500 high frequency LCR Meter is used along with a magnet up to 12 kOe and having accuracy of 10 Oe (provided by Marine India Electr. Pvt. Ltd).

3. Results and discussion

The substitution effects of Pr on the crystallization of BiFeO$_3$ samples were identified by XRD analysis. Figure 1 shows the XRD pattern of the BLPFO samples. All the samples crystallize in a rhombohedral distorted perovskite structure. Some extra peaks of $Bi_2Fe_4O_9$ and $Bi_{46}Fe_2O_{72}$ were also observed. It was reported earlier, that the substitution with moderate amount of rare earth ions in place of Bi^{3+} could eliminate the impurity phases in BiFeO$_3$ [8, 9]. Here also, the impurity peak in BLPFO-1 is weaker than that of undoped BiFeO$_3$, while no observable impurity peaks are observed in the XRD pattern of the BLPFO-2 samples. All the peaks for the BLPFO samples can be indexed according to the crystal structure of pure BiFeO$_3$. Careful inspection of the XRD pattern reveals that the peaks shift to larger 2θ values as the Pr content increases (shown in the inset of figure 1). This shift in the diffraction angle might be ascribed to the unit cell
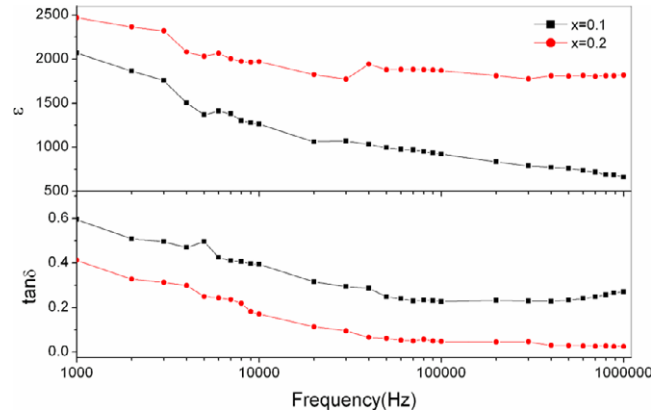
Figure 2. The variation of ε and tanδ with frequency for BLPFO-1 and BLPFO-2 samples at room temperature.

contraction or to the decrease in lattice constants due to the substitution of the smaller Pr^{3+} (1.126 Å) and Pr^{4+} (0.96 Å) ions as compared to Bi^{3+} (1.17 Å) ions. The calculated lattice parameters (equivalent hexagonal) of BLPFO are: for $x = 0.00$, $a = 5.5746$ Å, $c = 13.9831$ Å, for $x = 0.1$, $a = 5.5751$ Å, $c = 13.6640$ Å and for $x = 0.2$, $a = 5.5743$ Å, $c = 13.5946$ Å.

The frequency dependence of the dielectric constant (ε) and dielectric loss (tan δ) is shown in figure 2. In the low frequency range, both ε and tan δ have very high values. Both decrease gradually with the increase in frequency up to certain frequency (frequency sensitive region) and then they are nearly constant at high frequencies (frequency stable region). Space charge conduction is known to be an important contributor to tanδ at low frequencies. The room temperature dielectric constant (ε) increases with an increase in Pr content achieving a high value (above 2000) at 1000 Hz for the $x = 0.2$ composition. At the same time, increasing Pr content leads to a decrease in tan δ. This decrease in dissipation factor, tan δ, correlates with the corresponding changes in the electrical resistivities.

Figure 3 shows the temperature dependence of the dielectric constant (ε) for BLPFO system at different frequencies (1, 10 and 100 kHz). An abnormal diffuse dielectric pattern, containing an extremely high dielectric constant peak is observed for both BLPFO-1 and BLPFO-2 samples. The low temperature dielectric relaxation around $270\,^\circ$C found in BLPFO-1 is suppressed in the BLPFO-2. In the present system, the dopant oxide, Pr$_6$O$_{11}$ is known to have mixed oxidation states of 3+ and 4+ in oxides since it can be expressed as a mixture of Pr$_2$O$_3$ and PrO$_2$. It is expected that the high valence Pr^{4+} ion substitution for Bi^{3+} in BFO may reduce the oxygen vacancies. So we can infer that the low temperature diffuse peak is due to the point defects which will be reduced due to higher valence ions. There is another abnormality around $362\,^\circ$C in BLPFO-1. A sudden jump of the dielectric constant at $350\,^\circ$C for BLPFO-1 at 1 kHz is observed. This sudden jump could be attributed to a space charge contribution since this peak is not evident at higher frequencies. This peak is shifted to $312\,^\circ$C for BLPFO-2. Since BiFeO$_3$ shows an antiferromagnetic transition at $370\,^\circ$C
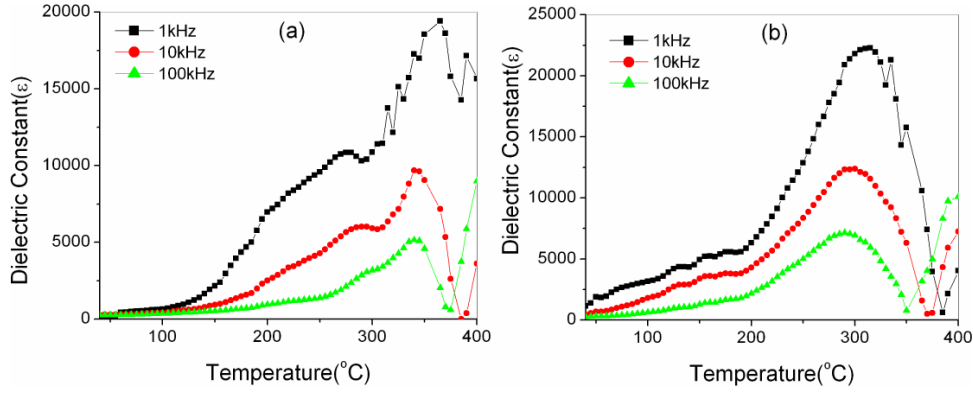
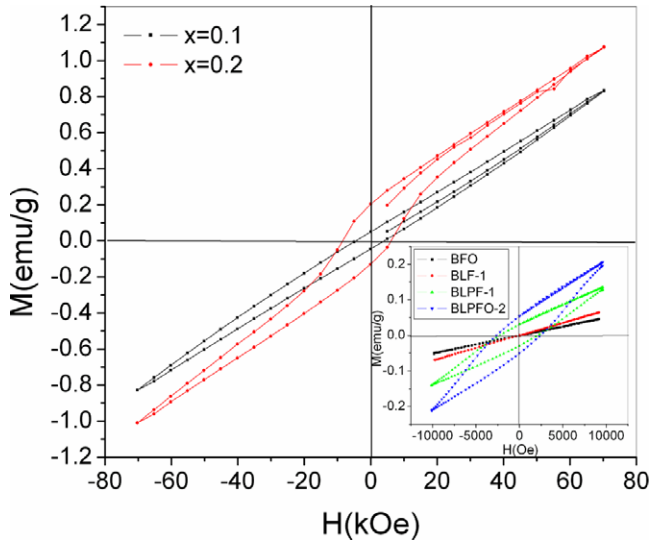**Figure 3.** Dielectric constant versus temperature plot for (a) BLPFO-1 and (b) BLPFO-2 samples.

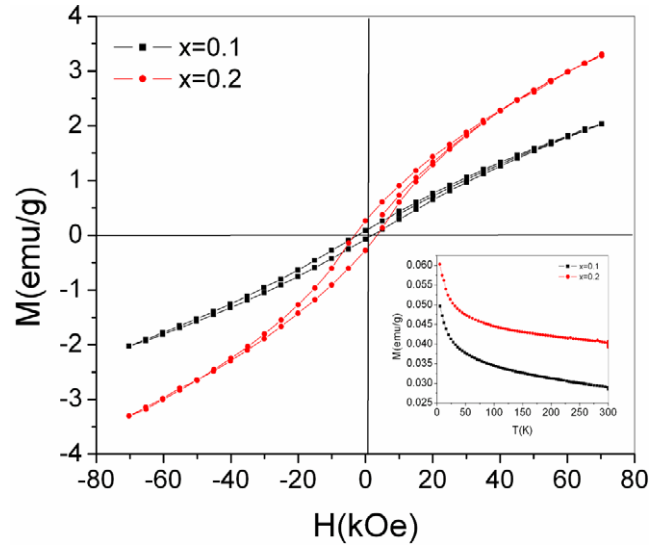**Figure 4.** Room temperature magnetic hysteresis plots for BLPFO-1 and BLPFO-2 samples.

Figure 5. M–H loops at 5 K for the BLPFO samples. The inset shows their M–T curves.

and a ferroelectric transition at 830 °C [1] and the observed peak at 312 °C is much lower than the ferroelectric transition, this peak could be related to the antiferromagnetic ordering Néel temperature (T_N). This type of dielectric anomaly is predicted by the Landau–Devonshire theory of phase transition in magnetoelectrically ordered systems as an influence of vanishing magnetic order on the electric order. The Landau free energy of a material can be written as (equation (1))

$$F(\vec{E}, \vec{H}) = \frac{\partial F}{\partial E_i} = F_0 - P_i^S E_i - M_i^S H_i$$
$$- \frac{1}{2}\varepsilon_0 \varepsilon_{ij} E_i E_j - \frac{1}{2}\mu_0 \mu_{ij} H_i H_j - \alpha_{ij} E_i H_j$$
$$- \frac{1}{2}\beta_{ijk} E_i H_j H_k - \frac{1}{2}\gamma_{ijk} H_i E_i E_j - \cdots. \quad (1)$$

From the above equation (1) we can derive the expression (equation (2)) of polarization

$$P_i(\vec{E}, \vec{H}) = -\frac{\partial F}{\partial E_i} = P_i^S + \varepsilon_0 \varepsilon_{ij} E_j + \alpha_{ij} H_j$$
$$+ \frac{1}{2}\beta_{ijk} H_j H_k + \gamma_{ijk} H_i E_j - \cdots. \quad (2)$$

where $\vec{P}^s$ denotes the spontaneous polarization, whereas $\hat{\varepsilon}$ and $\hat{\mu}$ are the electric and magnetic susceptibilities. The tensor $\hat{\alpha}$

corresponds to induction of polarization by a magnetic field or of magnetization by an electric field, which is designated as the linear ME effect, and higher order ME effects terms are parameterized by the tensors $\hat{\beta}$ and $\hat{\gamma}$.

Room temperature magnetization versus magnetic field (M–H) curves (figure 4) of BLPFO-1 and BLPFO-2 ceramics were measured with a magnetic field up to 70 kOe showing a weak hysteresis loop. The M–H loops show a maximum magnetization value of 1.1 emu g^{-1} and no tendency to saturate up to the maximum applied field of 7 T. We obtained a remnant magnetization of $2M_r = 0.0944$ emu g^{-1} and a coercivity of $2H_c = 8746$ Oe for the BLPFO-1 sample. For BLPFO-2, the $2M_r$ value increases to 0.3375 emu g^{-1} (3.57 times that of BLPFO-1) and $2H_c$ increases to 14 933 Oe. The inset shows the room temperature VSM measurements of pure BiFeO$_3$ (BFO), Bi$_{0.9}$La$_{0.1}$FeO$_3$ (BLFO), BLPFO-1 and BLPFO-2. It is clear that little enhancement in magnetization is seen for Bi$_{0.9}$La$_{0.1}$FeO$_3$ sample as compared to pure BiFeO$_3$. On the other hand the magnetization is increased by almost 4 times when P_r is co substituted at a Bi site. Hence Pr doping plays the dominant role towards the increase in magnetization.

3
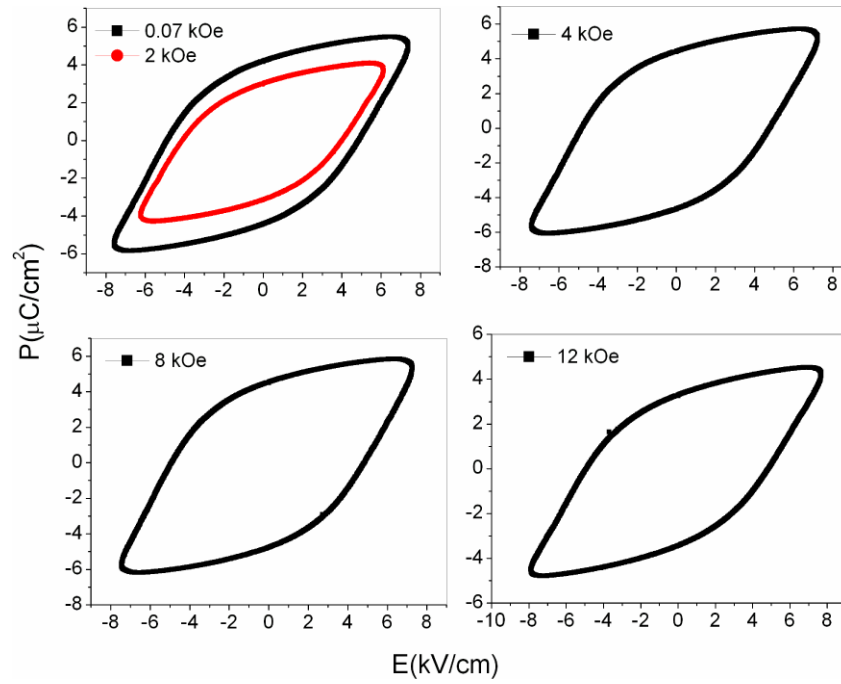
Figure 6. Ferroelectric (P–E) loops for a BLPFO-2 sample at different applied magnetic fields.
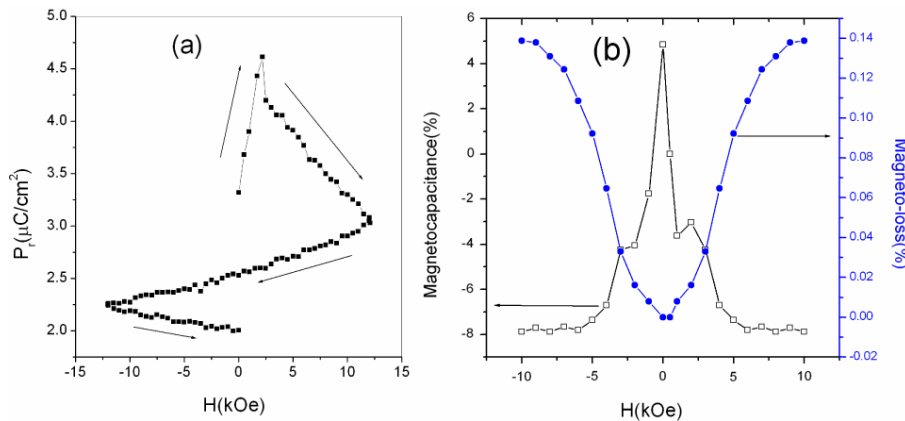
Figure 7. The variation of (a) P_r with the applied magnetic field. (b) shows the magnetocapacitance and magnetolosses as a function of magnetic field.

This increase in magnetization could be attributed to the substitution induced suppression of spiral spin structure. Also the magnetization behavior of our modified ceramic was found to be notably temperature dependent. Figure 5 shows the M–H response for the BLPFO ceramics taken at $T = 5$ K and the inset shows the temperature dependent magnetization for a moderate amount of applied field of 500 Oe so that the external field might not overshadow the intrinsic behavior of spins. The remnant magnetization was found to increase up to 1.63 times for both the samples on cooling to $T = 5$ K; however, the coercive field was decreased to half of the room temperature H_C values. This behavior is also observed in some high anisotropy magnetic materials such as MnBi [17]. A similar decrease in coercivity at low temperature has also been reported earlier in Nd doped $BiFeO_3$ and $BiFeO_3$–$BaTiO_3$ solid solution [18, 19]. Scott *et al* have reported magnetic anisotropy changes at low temperature in $BiFeO_3$. Below room

temperature it undergoes spin reorientation transitions at $T2 = 200$ K and $T1 = 140$ K. Between $T1$ and $T2$ the magnetic symmetry is very low and hence the system shows a linear magnetoelectric effect. These transitions are related to spin frustration [20]. Hence this decrease in magnetic coercivity (H_c) could be attributed to magnetic anisotropy changes at low temperatures. In order to study the magnetoelectric coupling, we measured the P–E loops at room temperature under different applied magnetic fields. We first took the P–E loop without applying a magnetic field and then we increased the magnetic field in steps of 0.5 kOe and measured the P–E loops at each step. The maximum applied field was 12 kOe. Then we started decreasing the field to 0 Oe. Then we performed the same measurement by reversing the magnetic field. It is well known that well saturated ferroelectric loops in undoped $BiFeO_3$ have been difficult to obtain due to the inherently high coercive field and low resistivity [21, 22]. Since the resistivity

of $BiFeO_3$ increases with Pr doping, we obtained hysteresis ($P–E$) loops for Pr doped $BiFeO_3$ samples, though the shape of the polarization–electric field ($P–E$) loops was not a classical ferroelectric type. Figure 6 shows the $P–E$ loops of BLPFO-2 samples taken at various magnetic fields when the field was increased stepwise. At the same applied electric field, the remnant polarization (P_r) was found to vary with the intensity of the magnetic field. The variation of P_r with the applied magnetic field is shown in figure 7(a). The values first increases from 3.32 to 4.6 μC cm^{-2} as the magnetic field increased from 0.07 to 2 kOe. With a further increase in magnetic field the P_r values decrease continuously to 2.58 μC cm^{-2} at the end of the cycle. The polarization is further decreased when the magnetic field is reversed. We measured the capacitance and dielectric loss at a frequency of 1 kHz as a function of magnetic field ranging from -9 to 9 kOe. The magnetocapacitance measurements are shown in figure 7(b).

The magnetocapacitance is defined as (equation (3))

$$MC = \frac{\varepsilon'(H) - \varepsilon'(0)}{\varepsilon'(0)} \times 100 \qquad (3)$$

and the magnetolosses, defined as (equation (4))

$$ML = \frac{\tan\delta(H) - \tan\delta(0)}{\tan\delta(0)} \times 100. \qquad (4)$$

A similar type of observation was earlier reported by Catalan *et al* for $BiMnO_3$ materials [23]. In our case the magnetocapacitance is relatively smaller.

Here the dielectric constant is found to decrease suddenly up to 2 kOe. In general a dielectric anomaly indicates a sudden change of polarization (rotation etc) [24]. From these results, one can see a strong magnetoelectric coupling in the system. The cause for this coupling is inherent in the $BiFeO_3$ system itself. $BiFeO_3$ has its antiferromagnetic axis oriented along the [110] and its electric polarization directed along one of the equivalent [111] directions. The ferroelectricity is accompanied by a ferroelastic strain resulting from distortion of the lattice. Switching of the polarization is accompanied by switching of the ferroelastic domain state. The orientation of the antiferromagnetic sublattice magnetization is coupled to the ferroelastic strain state in $BiFeO_3$, which should always be perpendicular to the ferroelectric polarization. Therefore, electric polarization switching will lead to a reorientation of the antiferromagnetic ordered spins. Conversely, a transition from the spin disordered state to the spin ordered antiferromagnetic state will affect the ferroelastic domain state and eventually disturb the ordered electric dipoles. Hence in the present system, the applied magnetic field has changed the ferroelectric property via the ferroelasticity of the system.

4. Conclusion

Pure and Pr substituted $BiFeO_3$ polycrystalline ceramics were synthesized using a solid state reaction route. Pr substitution at a Bi site eliminated the small usual impurity phase in $BiFeO_3$ and stabilized the crystal structure. The dielectric properties were enhanced by Pr substitution i.e. ε is increased to 1000 for 100 Hz with a considerable decrease in tan δ (0.4 for 100 Hz). A systematic increase in both the ferroelectric and ferromagnetic properties was achieved. The observed increase in the magnetic parameters H_c and M_r (1.7% and 3.5% respectively) with an increase in Pr doping reflect the corresponding increase in the suppression of spin spiral with a continual change in lattice parameters. The coexistence of ferromagnetism and ferroelectricity has been confirmed in the bulk materials of Pr doped $BiFeO_3$ by means of $M–H$ and $P–E$ loop measurements. We have also shown magnetodielectric measurements at room temperature. Direct observation of the P_r dependence on the magnetic field is the most conclusive experimental evidence of magnetoelectric coupling in this novel system.

References

[1]　Hill N A 2000 *J. Phys. Chem.* B **104** 6694
[2]　Fiebig M 2005 *J. Phys. D: Appl. Phys.* **38** R123
[3]　Sosnowska I, Peterlin-Neumaier T and Streichele E 1982 *J. Phys. C: Solid State Phys.* **15** 4835
[4]　Kubel F and Schmid H 1990 *Acta Crystallogr.* B **46** 698
[5]　Michel C, Moreau J M, Achenbach G D, Gerson R and James W J 1969 *Solid State Commun.* **7** 701
[6]　Li M, Ning M, Ma Y, Wu Q and Ong C K 2007 *J. Phys. D: Appl. Phys.* **40** 1603
[7]　Kumar M and Yadav K L 2006 *J. Appl. Phys.* **100** 074111
[8]　Uniyal P and Yadav K L 2009 *J. Appl. Phys.* **105** 07D914
[9]　Uniyal P and Yadav K L 2009 *J. Phys.: Condens. Matter* **21** 012205
[10]　Lee Y-H, Wu J-M and Lai C-H 2006 *Appl. Phys. Lett.* **88** 042903
[11]　Bhushan B, Basumallick A, Bandopadhyay S K, Vasanthacharya N Y and Das D 2009 *J. Phys. D: Appl. Phys.* **42** 065004
[12]　Wang J, Zheng H, Nagarajan V, Liu B, Ogale S B, Viehland D, Venugopalan V, Schlom D G, Wuttig M, Ramesh R, Neaton J B, Waghmare U V, Hill N A and Rabe K M 2003 *Science* **299** 1719
[13]　Uniyal P and Yadav K L 2008 *Mater. Lett.* **62** 2858
[14]　Wang J, Neaton J B, Zheng H, Nagarajan V, Ogale S B, Liu B, Viehland D, Vaithyanathan V, Schlom D G, Waghmare U V, Spaldin N A, Rabe K M, Wuttig M and Ramesh R 2003 *Science* **299** 1719
[15]　Yu B, Li M, Hu Z, Pei L, Guo D, Zhao X and Dong S 2008 *Appl. Phys. Lett.* **93** 182909
[16]　Palkar V R, Kundaliya D C, Malik S K and Bhattacharya S 2004 *Phys. Rev.* B **69** 212102
[17]　Yang J B, Yelon W B, James W J, Cai Q, Kornecki M, Roy S, Ali N and l'Heritier Ph 2002 *J. Phys.: Condens. Matter* **14** 6509
[18]　Mishra R K, Pradhan D K, Choudhary R N P and Banerjee A 2008 *J. Magn. Magn. Mater.* **320** 2602
[19]　Mahesh Kumar M, Srinath S, Kumar G S and Suryanarayana S V 1998 *J. Magn. Magn. Mater.* **188** 203
[20]　Scott J F 2009 *J. Magn. Magn. Mater.* **321** 1689
[21]　Dawber M, Rabe K M and Scott J F 2005 *Rev. Mod. Phys.* **77** 1083

[22] Kharel P, Talebi S, Ramachandran B, Dixit A, Naik V M,
     Sahana1 M B, Sudakar C, Naik R, Rao M S R and
     Lawes G 2009 *J. Phys.: Condens. Matter* **21** 036001

[23] Catalan G 2006 *Appl. Phys. Lett.* **88** 102902
[24] Hur N, Park S, Sharma P A, Ahn J S, Guha S and
     Cheong S-W 2004 *Nature* **429** 392